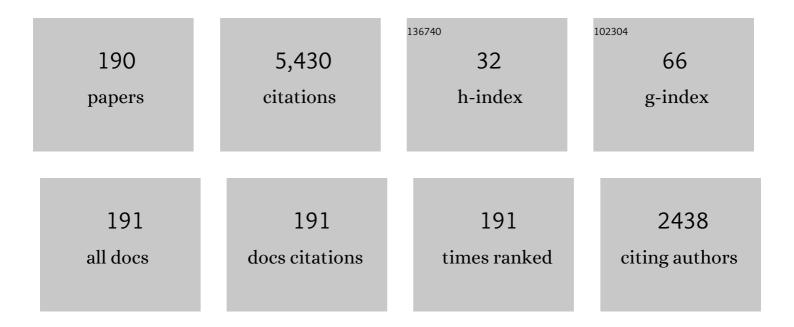
Andreas Kirschner

List of Publications by Year in descending order

Source: https://exaly.com/author-pdf/3934198/publications.pdf Version: 2024-02-01



#	Article	IF	CITATIONS
1	Latest results of Eurofusion plasma-facing components research in the areas of power loading, material erosion and fuel retention. Nuclear Fusion, 2022, 62, 042013.	1.6	11
2	Operating a full tungsten actively cooled tokamak: overview of WEST first phase of operation. Nuclear Fusion, 2022, 62, 042007.	1.6	39
3	Experimental confirmation of efficient island divertor operation and successful neoclassical transport optimization in Wendelstein 7-X. Nuclear Fusion, 2022, 62, 042022.	1.6	24
4	Beryllium erosion and redeposition in ITER H, He and D–T discharges. Nuclear Fusion, 2022, 62, 036011.	1.6	13
5	Predictive 3D modelling of erosion and deposition in ITER with ERO2.0: from beryllium main wall, tungsten divertor to full-tungsten device. Physica Scripta, 2022, 97, 014001.	1.2	2
6	Simulation Analysis of the Carbon Deposition Profile on Directional Material Probes in the Large Helical Device Using the ERO2.0 Code. Plasma and Fusion Research, 2022, 17, 2403010-2403010.	0.3	1
7	Simulation of Impurity Transport and Deposition in the Closed Helical Divertor in the Large Helical Device. Plasma and Fusion Research, 2021, 16, 2403004-2403004.	0.3	2
8	A sensitivity analysis of numerical predictions for beryllium erosion and migration in ITER. Nuclear Materials and Energy, 2021, 26, 100904.	0.6	9
9	Symmetries of 13C tracer deposition in EAST D and He plasmas investigated on the sub-mm to 100 mm scale by deuteron nuclear reaction analysis. Fusion Engineering and Design, 2021, 166, 112292.	1.0	1
10	The impact of surface morphology on the erosion of metallic surfaces – Modelling with the 3D Monte-Carlo code ERO2.0. Nuclear Materials and Energy, 2021, 27, 100987.	0.6	9
11	Interpretative modeling of impurity transport and tungsten sources in WEST boundary plasma. Nuclear Fusion, 2021, 61, 126015.	1.6	4
12	Effectiveness of local methane and hydrogen injection into the scrape-off layer of W7-X by means of the multi-purpose manipulator. Fusion Engineering and Design, 2021, 173, 112786.	1.0	1
13	Plasma-wall interaction studies in W7-X: main results from the recent divertor operations. Physica Scripta, 2021, 96, 124059.	1.2	10
14	13C tracer deposition in EAST D and He plasmas investigated by high-throughput deuteron nuclear reaction analysis mapping. Nuclear Materials and Energy, 2020, 25, 100805.	0.6	7
15	Boron transport simulation using the ERO2.0 code for real-time wall conditioning in the large helical device. Nuclear Materials and Energy, 2020, 25, 100853.	0.6	4
16	Erosion and screening of tungsten during inter/intra-ELM periods in the JET-ILW divertor. Nuclear Materials and Energy, 2020, 25, 100859.	0.6	7
17	ERO2.0 modelling of the effects of surface roughness on molybdenum erosion and redeposition in the PSI-2 linear plasma device. Physica Scripta, 2020, T171, 014057.	1.2	19
18	First Monteâ€Carlo modelling of global beryllium migration in ITER using ERO2.0. Contributions To Plasma Physics, 2020, 60, e201900149.	0.5	17

#	Article	IF	CITATIONS
19	First efforts in numerical modeling of tungsten migration in WEST with SolEdge2D-EIRENE and ERO2.0. Physica Scripta, 2020, T171, 014013.	1.2	16
20	Fuel inventory and impurity deposition in castellated tungsten tiles in KSTAR: experiment and modelling. Physica Scripta, 2020, T171, 014049.	1.2	2
21	First divertor physics studies in Wendelstein 7-X. Nuclear Fusion, 2019, 59, 096014.	1.6	34
22	Overview of first Wendelstein 7-X high-performance operation. Nuclear Fusion, 2019, 59, 112004.	1.6	165
23	Erosion, screening, and migration of tungsten in the JET divertor. Nuclear Fusion, 2019, 59, 096035.	1.6	60
24	Modelling of tungsten erosion and deposition in the divertor of JET-ILW in comparison to experimental findings. Nuclear Materials and Energy, 2019, 18, 239-244.	0.6	24
25	Beryllium global erosion and deposition at JET-ILW simulated with ERO2.0. Nuclear Materials and Energy, 2019, 18, 331-338.	0.6	36
26	Improved ERO modelling of beryllium erosion at ITER upper first wall panel using JET-ILW and PISCES-B experience. Nuclear Materials and Energy, 2019, 19, 510-515.	0.6	15
27	Physics affecting heavy impurity migration in tokamaks: Benchmarking test-ion code ASCOT against TEXTOR tracer experiment. Nuclear Materials and Energy, 2019, 19, 307-315.	0.6	1
28	Surface roughness effect on Mo physical sputtering and re-deposition in the linear plasma device PSI-2 predicted by ERO2.0. Nuclear Materials and Energy, 2019, 19, 13-18.	0.6	27
29	Determination of tungsten sources in the JET-ILW divertor by spectroscopic imaging in the presence of a strong plasma continuum. Nuclear Materials and Energy, 2019, 18, 118-124.	0.6	16
30	ERO modeling and sensitivity analysis of locally enhanced beryllium erosion by magnetically connected antennas. Nuclear Fusion, 2018, 58, 016046.	1.6	9
31	Modelling of plasma-wall interaction and impurity transport in fusion devices and prompt deposition of tungsten as application. Plasma Physics and Controlled Fusion, 2018, 60, 014041.	0.9	31
32	Review on global migration, fuel retention and modelling after TEXTOR decommission. Nuclear Materials and Energy, 2018, 17, 83-112.	0.6	9
33	Surface roughness effects on plasma near a divertor plate and local impact angle. Nuclear Materials and Energy, 2017, 12, 313-317.	0.6	9
34	Modelling of deposition and erosion of injected WF6 and MoF6 in TEXTOR. Nuclear Materials and Energy, 2017, 12, 564-568.	0.6	4
35	Whole-machine material migration studies in the TEXTOR tokamak with molybdenum. Nuclear Materials and Energy, 2017, 12, 518-523.	0.6	6
36	Advances in understanding of high- <i>Z</i> material erosion and re-deposition in low- <i>Z</i> wall environment in DIII-D. Nuclear Fusion, 2017, 57, 056016.	1.6	16

#	Article	IF	CITATIONS
37	High-Z material erosion and its control in DIII-D carbon divertor. Nuclear Materials and Energy, 2017, 12, 247-252.	0.6	4
38	Fuel inventory and deposition in castellated structures in JET-ILW. Nuclear Fusion, 2017, 57, 066027.	1.6	25
39	ERO modelling of tungsten erosion and re-deposition in EAST L mode discharges. Physics of Plasmas, 2017, 24, 092512.	0.7	20
40	Quartz micro-balance results of pulse-resolved erosion/deposition in the JET-ILW divertor. Nuclear Materials and Energy, 2017, 12, 478-482.	0.6	6
41	Overview of wall probes for erosion and deposition studies in the TEXTOR tokamak. Matter and Radiation at Extremes, 2017, 2, 87-104.	1.5	23
42	ERO modelling of tungsten erosion in the linear plasma device PSI-2. Nuclear Materials and Energy, 2017, 12, 253-260.	0.6	21
43	ERO modeling of beryllium erosion by helium plasma in experiments at PISCES-B. Nuclear Materials and Energy, 2017, 12, 1157-1162.	0.6	7
44	ERO modeling of Cr sputtering in the linear plasma device PSI-2. Physica Scripta, 2017, T170, 014051.	1.2	4
45	Experimental data on low energy electron impact ionisation of W. Physica Scripta, 2017, T170, 014075.	1.2	1
46	Numerical and analytic study of rough surface morphology on the angular distribution of eroded impurity. Contributions To Plasma Physics, 2017, 57, 329-335.	0.5	7
47	An analytical expression for ion velocities at the wall including the sheath electric field and surface biasing for erosion modeling at JET ILW. Nuclear Materials and Energy, 2017, 12, 341-345.	0.6	10
48	First ERO2.0 modeling of Be erosion and non-local transport in JET ITER-like wall. Physica Scripta, 2017, T170, 014018.	1.2	27
49	Plasma-wall interactions in the presence of plasma fluctuations—interpretation of line emission from sputtered tungsten in PSI-2. Physica Scripta, 2017, T170, 014039.	1.2	3
50	Plasma–wall interaction studies within the EUROfusion consortium: progress on plasma-facing components development and qualification. Nuclear Fusion, 2017, 57, 116041.	1.6	75
51	Experimental estimation of tungsten impurity sputtering due to Type I ELMs in JET-ITER-like wall using pedestal electron cyclotron emission and target Langmuir probe measurements. Physica Scripta, 2016, T167, 014005.	1.2	31
52	Three-dimensional modeling of plasma edge transport and divertor fluxes during application of resonant magnetic perturbations on ITER. Nuclear Fusion, 2016, 56, 066008.	1.6	34
53	An Analytical Expression for the Electric Field and Particle Tracing in Modelling of Be Erosion Experiments at the JET ITERâ€like Wall. Contributions To Plasma Physics, 2016, 56, 640-645.	0.5	26
54	Improved ERO modelling for spectroscopy of physically and chemically assisted eroded beryllium from the JET-ILW. Nuclear Materials and Energy, 2016, 9, 604-609.	0.6	17

#	Article	IF	CITATIONS
55	Modelling of Impurity Transport and Plasma–Wall Interaction in Fusion Devices with the ERO Code: Basics of the Code and Examples of Application. Contributions To Plasma Physics, 2016, 56, 622-627.	0.5	21
56	Deposition in the inner and outer corners of the JET divertor with carbon wall and metallic ITER-like wall. Physica Scripta, 2016, T167, 014052.	1.2	14
57	Estimates of RF-induced erosion at antenna-connected beryllium plasma-facing components in JET. Physica Scripta, 2016, T167, 014035.	1.2	14
58	Simulation of gross and net erosion of high-Z materials in the DIII-D divertor. Nuclear Fusion, 2016, 56, 016021.	1.6	41
59	Local migration studies of high-Zmetals in the TEXTOR tokamak. Physica Scripta, 2016, T167, 014058.	1.2	9
60	Modelling of the material transport and layer formation in the divertor of JET: Comparison of ITER-like wall with full carbon wall conditions. Journal of Nuclear Materials, 2015, 463, 116-122.	1.3	26
61	Analysis of rotating collectors from the private region of JET with carbon wall and metallic ITER-like wall. Journal of Nuclear Materials, 2015, 463, 818-821.	1.3	9
62	Modelling the erosion/deposition pattern of the Tore Supra Toroidal Pumped Limiter. Journal of Nuclear Materials, 2015, 463, 827-831.	1.3	1
63	Material deposition on inner divertor quartz-micro balances during ITER-like wall operation in JET. Journal of Nuclear Materials, 2015, 463, 796-799.	1.3	8
64	Preliminary Monte Carlo simulation of beryllium migration during JET ITER-like wall divertor operation. Journal of Nuclear Materials, 2015, 463, 800-804.	1.3	3
65	Beryllium migration in JET ITER-like wall plasmas. Nuclear Fusion, 2015, 55, 063021.	1.6	83
66	Material migration studies with an ITER first wall panel proxy on EAST. Nuclear Fusion, 2015, 55, 023013.	1.6	35
67	Modeling of tungsten transport in the linear plasma device PSI-2 with the 3D Monte-Carlo code ERO. Journal of Nuclear Materials, 2015, 463, 268-271.	1.3	7
68	Kinetic modelling of material erosion and impurity transport in edge localized modes in EAST. Nuclear Fusion, 2015, 55, 043003.	1.6	16
69	Ion target impact energy during Type I edge localized modes in JET ITER-like Wall. Plasma Physics and Controlled Fusion, 2015, 57, 085006.	0.9	44
70	Modelling of surface evolution of rough surface on divertor target in fusion devices. Journal of Nuclear Materials, 2015, 463, 372-376.	1.3	16
71	Erosion/re-deposition modeling in an ITER divertor-like high-density, low-temperature plasma beam. Plasma Physics and Controlled Fusion, 2014, 56, 095028.	0.9	1
72	Modelling of surface roughness effects on impurity erosion and deposition in TEXTOR with a code package SURO/ERO/SDPIC. Nuclear Fusion, 2014, 54, 123015.	1.6	17

#	Article	IF	CITATIONS
73	Estimation of the contribution of gaps to tritium retention in the divertor of ITER. Physica Scripta, 2014, T159, 014063.	1.2	4
74	First results from the ¹⁰ Be marker experiment in JET with ITER-like wall. Nuclear Fusion, 2014, 54, 082004.	1.6	4
75	Study of physical and chemical assisted physical sputtering of beryllium in the JET ITER-like wall. Nuclear Fusion, 2014, 54, 103001.	1.6	55
76	Removable samples for ITER—a feasibility and conceptual study. Physica Scripta, 2014, T159, 014004.	1.2	6
77	Determination of Be sputtering yields from spectroscopic observations at the JET ITER-like wall based on three-dimensional ERO modelling. Physica Scripta, 2014, T159, 014057.	1.2	21
78	Simulation of spectroscopic patterns obtained in W/C test-limiter sputtering experiment at TEXTOR. Journal of Nuclear Materials, 2013, 438, S351-S355.	1.3	6
79	Kinetic effects of inclined magnetic field on physical sputtering by impurity ions. Journal of Nuclear Materials, 2013, 438, S909-S912.	1.3	10
80	Improved carbon migration modelling with the ERO code. Journal of Nuclear Materials, 2013, 438, S891-S894.	1.3	2
81	Material deposition and migration processes with resonant magnetic perturbation fields at TEXTOR. Journal of Nuclear Materials, 2013, 438, S602-S606.	1.3	5
82	Carbon transport and escape fraction in a high density plasma beam. Journal of Nuclear Materials, 2013, 438, S629-S632.	1.3	5
83	Carbon deposition at the bottom of gaps in TEXTOR experiments. Journal of Nuclear Materials, 2013, 438, S775-S779.	1.3	5
84	Modelling of lithium erosion and transport in FTU lithium experiments. Journal of Nuclear Materials, 2013, 438, S690-S693.	1.3	9
85	Spectroscopic measurements of Be erosion at JET ILW and interpretation with ERO modelling. Journal of Nuclear Materials, 2013, 438, S267-S271.	1.3	26
86	Modeling of divertor particle and heat loads during application of resonant magnetic perturbation fields for ELM control in ITER. Journal of Nuclear Materials, 2013, 438, S194-S198.	1.3	25
87	Studies of impurity migration in TEXTOR by local tracer injection. Journal of Nuclear Materials, 2013, 438, S723-S726.	1.3	9
88	Multiscale modeling of BeD release and transport in PISCES-B. Journal of Nuclear Materials, 2013, 438, S276-S279.	1.3	15
89	Molecules can be sputtered also from pure metals: sputtering of beryllium hydride by fusion plasma–wall interactions. Plasma Physics and Controlled Fusion, 2013, 55, 074004.	0.9	29
90	Modelling of local carbon deposition on a rough test limiter exposed to the edge plasma of TEXTOR. Plasma Physics and Controlled Fusion, 2013, 55, 055004.	0.9	12

#	Article	IF	CITATIONS
91	Global migration of impurities in tokamaks. Plasma Physics and Controlled Fusion, 2013, 55, 124029.	0.9	15
92	Modeling of Impurity Transport in the Divertor of JET. Plasma and Fusion Research, 2013, 8, 2402038-2402038.	0.3	1
93	Dissociative recombination and electron-impact de-excitation in CH photon emission under ITER divertor-relevant plasma conditions. Plasma Physics and Controlled Fusion, 2012, 54, 095013.	0.9	15
94	Outer divertor of ASDEX Upgrade in low-density L-mode discharges in forward and reversed magnetic field: II. Analysis of local impurity migration. Nuclear Fusion, 2012, 52, 103007.	1.6	7
95	Erosion and Deposition Mechanisms in Fusion Plasmas. Fusion Science and Technology, 2012, 61, 230-245.	0.6	2
96	Simulation of hydrogen retention and re-emission from tungsten exposed to divertor plasmas. Physica Scripta, 2011, T145, 014047.	1.2	2
97	Modelling of carbon deposition from CD ₄ injection in the far scrape-off layer of TEXTOR. Physica Scripta, 2011, T145, 014005.	1.2	3
98	ERO code benchmarking of ITER first wall beryllium erosion/re-deposition against LIM predictions. Physica Scripta, 2011, T145, 014008.	1.2	38
99	Passive protection of the ITER diagnostic mirrors. Physica Scripta, 2011, T145, 014071.	1.2	10
100	Studies of the influence of external hydrocarbon injection on local plasma conditions and resulting carbon transport. Journal of Nuclear Materials, 2011, 415, S270-S273.	1.3	6
101	PIC simulation of kinetic effects of plasma and consequences for physical sputtering. Journal of Nuclear Materials, 2011, 415, S192-S195.	1.3	4
102	Deposition and re-erosion studies by means of local impurity injection in TEXTOR. Journal of Nuclear Materials, 2011, 415, S239-S245.	1.3	25
103	Effect of E×B driven transport on the deposition of carbon in the outer divertor of ASDEX Upgrade. Journal of Nuclear Materials, 2011, 415, S231-S234.	1.3	12
104	Analysis of the local re-deposition behavior of carbon at the main walls in TEXTOR by CD4 gas injection and Quartz Microbalance techniques. Journal of Nuclear Materials, 2011, 415, S246-S249.	1.3	1
105	Induced carbon deposition by local hydrocarbon injection into detached divertor plasmas in JET. Journal of Nuclear Materials, 2011, 415, S235-S238.	1.3	1
106	Simulation of Be–C interaction dynamics in mixed Be/C layers formed in experiments at PISCES-B. Journal of Nuclear Materials, 2011, 415, S219-S222.	1.3	10
107	Overview of material migration and mixing, fuel retention and cleaning of ITER-like castellated structures in TEXTOR. Journal of Nuclear Materials, 2011, 415, S289-S292.	1.3	20
108	Quantification of chemical erosion in the DIII-D divertor and implications for ITER. Journal of Nuclear Materials, 2011, 415, S141-S144.	1.3	2

#	Article	IF	CITATIONS
109	Multi machine scaling of fuel retention in 4 carbon dominated tokamaks. Journal of Nuclear Materials, 2011, 415, S735-S739.	1.3	20
110	Particle-in-cell simulations of plasma interaction with shaped and unshaped gaps in TEXTOR. Plasma Physics and Controlled Fusion, 2011, 53, 115004.	0.9	18
111	Erosion and Deposition Mechanisms in Fusion Plasmas. Fusion Science and Technology, 2010, 57, 277-292.	0.6	5
112	Modelling of Impurity Transport in the Linear Plasma Devices PISCESâ€B and Pilotâ€PSI Using the Monte arlo Code ERO. Contributions To Plasma Physics, 2010, 50, 432-438.	0.5	17
113	Modelling of Carbon Transport in the Outer Divertor Plasma of ASDEX Upgrade. Contributions To Plasma Physics, 2010, 50, 439-444.	0.5	6
114	Analysis of Carbon Deposition on the FirstWall of LHD by Monte Carlo Simulation. Contributions To Plasma Physics, 2010, 50, 451-457.	0.5	5
115	Molecular dynamics and dynamic Monte Carlo studies of mixed materials and their impact on plasma wall interactions. Fusion Engineering and Design, 2010, 85, 1167-1172.	1.0	10
116	Modelling of local carbon deposition from methane and ethene injection through graphite and tungsten test limiters in TEXTOR. Plasma Physics and Controlled Fusion, 2010, 52, 045005.	0.9	7
117	Modelling of impurity deposition in gaps of castellated surfaces with the 3D-GAPS code. Plasma Physics and Controlled Fusion, 2010, 52, 075007.	0.9	29
118	Determination of rate coefficients for fusion-relevant atoms and molecules by modelling and measurement in the boundary layer of TEXTOR. Journal of Physics B: Atomic, Molecular and Optical Physics, 2010, 43, 144017.	0.6	47
119	Nonlinear Impact of Edge Localized Modes on Carbon Erosion in the Divertor of the JET Tokamak. Physical Review Letters, 2009, 102, 045007.	2.9	27
120	Simulation of light emission from hydrocarbon injection in TEXTOR using the ERO code. Plasma Physics and Controlled Fusion, 2009, 51, 055019.	0.9	12
121	Castellated structures for ITER: Differences of impurity deposition and fuel accumulation in the toroidal and poloidal gaps. Journal of Nuclear Materials, 2009, 386-388, 809-812.	1.3	7
122	Effects of tungsten surface conditions on carbon deposition. Journal of Nuclear Materials, 2009, 390-391, 44-48.	1.3	19
123	Investigations of castellated structures for ITER: The effect of castellation shaping and alignment on fuel retention and impurity deposition in gaps. Journal of Nuclear Materials, 2009, 390-391, 556-559.	1.3	32
124	Modelling of Be transport in PSI experiments at PISCES-B. Journal of Nuclear Materials, 2009, 390-391, 106-109.	1.3	8
125	Simulation of redeposition of carbon/hydrocarbon on a material surface with castellated structures. Journal of Nuclear Materials, 2009, 390-391, 119-122.	1.3	10
126	Estimations of erosion fluxes, material deposition and tritium retention in the divertor of ITER. Journal of Nuclear Materials, 2009, 390-391, 152-155.	1.3	36

#	Article	IF	CITATIONS
127	Improvement of surface processes modelling in the ERO code. Journal of Nuclear Materials, 2009, 390-391, 175-178.	1.3	2
128	Numerical modelling of steady-state fluxes at the ITER first wall. Journal of Nuclear Materials, 2009, 390-391, 528-531.	1.3	23
129	Recent analysis of key plasma wall interactions issues for ITER. Journal of Nuclear Materials, 2009, 390-391, 1-9.	1.3	671
130	Simulation of hydrocarbon reflection from carbon and tungsten surfaces and its impact on codeposition patterns on plasma facing components. Journal of Nuclear Materials, 2009, 390-391, 72-75.	1.3	24
131	Modeling of erosion and deposition by the Monte Carlo codes EDDY and ERO. Physica Scripta, 2009, T138, 014010.	1.2	7
132	Prediction of long-term tritium retention in the divertor of ITER: influence of modelling assumptions on retention rates. Physica Scripta, 2009, T138, 014011.	1.2	18
133	Chemical erosion of different carbon composites under ITER-relevant plasma conditions. Physica Scripta, 2009, T138, 014017.	1.2	16
134	ERO modelling of local deposition of injected13C tracer at the outer divertor of JET. Physica Scripta, 2009, T138, 014021.	1.2	6
135	Comparison of13C2H4and13CH4injection through graphite and tungsten limiters in TEXTOR. Physica Scripta, 2009, T138, 014022.	1.2	6
136	Progress in Edge Plasma Transport Modeling on JET. Contributions To Plasma Physics, 2008, 48, 190-195.	0.5	3
137	Effect of surface roughness and substrate material on carbon erosion and deposition in the TEXTOR tokamak. Plasma Physics and Controlled Fusion, 2008, 50, 095008.	0.9	47
138	Modelling of13CH4injection experiments with graphite and tungsten test limiters in TEXTOR using the coupled code ERO-SDTrimSP. Plasma Physics and Controlled Fusion, 2008, 50, 015006.	0.9	31
139	Modelling of carbon migration during JET13C injection experiments. Nuclear Fusion, 2008, 48, 105002.	1.6	29
140	Erosion and Deposition Mechanisms in Fusion Plasmas. Fusion Science and Technology, 2008, 53, 259-277.	0.6	5
141	Modelling of chemical erosion mitigation experiments at PISCES-B using the 3D Monte-Carlo code ERO. Physica Scripta, 2007, T128, 127-132.	1.2	15
142	Chapter 4: Power and particle control. Nuclear Fusion, 2007, 47, S203-S263.	1.6	891
143	Modelling of tritium retention and target lifetime of the ITER divertor using the ERO code. Journal of Nuclear Materials, 2007, 363-365, 91-95.	1.3	56
144	Study of local carbon transport on graphite, tungsten and molybdenum test limiters in TEXTOR by 13CH4 tracer injection. Journal of Nuclear Materials, 2007, 363-365, 179-183.	1.3	25

#	Article	IF	CITATIONS
145	The effect of the magnetic topology on particle recycling in the ergodic divertor of TEXTOR. Journal of Nuclear Materials, 2007, 363-365, 377-381.	1.3	2
146	Diagnostic mirrors for ITER: A material choice and the impact of erosion and deposition on their performance. Journal of Nuclear Materials, 2007, 363-365, 1395-1402.	1.3	94
147	Carbon transport, deposition and fuel accumulation in castellated structures exposed in TEXTOR. Journal of Nuclear Materials, 2007, 367-370, 1481-1486.	1.3	25
148	Long-term erosion and deposition studies of the main graphite limiter in TEXTOR. Physica Scripta, 2007, T128, 35-39.	1.2	5
149	Castellated structures for ITER: the influence of the shape of castellation on the impurity deposition and fuel accumulation in gaps. Physica Scripta, 2007, T128, 45-49.	1.2	10
150	Tritium retention in next step devices and the requirements for mitigation and removal techniques. Plasma Physics and Controlled Fusion, 2006, 48, B189-B199.	0.9	83
151	Impurity Transport Modelling in Edge Plasmas of Fusion Devices with the Monte Carlo Code ERO. Contributions To Plasma Physics, 2006, 46, 628-634.	0.5	13
152	Investigation of carbon transport by13CH4injection through graphite and tungsten test limiters in TEXTOR. Plasma Physics and Controlled Fusion, 2006, 48, 1401-1412.	0.9	29
153	Overview of Erosion Mechanisms, Impurity Transport, and Deposition in TEXTOR and Related Modeling. Fusion Science and Technology, 2005, 47, 146-160.	0.6	7
154	Mixed and High-Z Plasma-Facing Materials in TEXTOR. Springer Series in Chemical Physics, 2005, , 319-333.	0.2	2
155	Carbon chemical erosion in H-mode discharges in ASDEX Upgrade divertor IIb: flux dependence and local redeposition. Journal of Nuclear Materials, 2005, 337-339, 985-989.	1.3	17
156	Experimental observations and modelling of carbon transport in the inner divertor of JET. Journal of Nuclear Materials, 2005, 337-339, 17-24.	1.3	17
157	Identification of molecular carbon sources in the JET divertor by means of emission spectroscopy. Journal of Nuclear Materials, 2005, 337-339, 1058-1063.	1.3	33
158	Flux dependence of carbon erosion and implication for ITER. Journal of Nuclear Materials, 2005, 337-339, 970-974.	1.3	90
159	Dynamic transition between erosion and deposition on a tungsten surface exposed to edge plasmas containing carbon impurities. Journal of Nuclear Materials, 2005, 337-339, 882-886.	1.3	9
160	Report on the 11th European Fusion Physics Workshop (Heraklion, Crete, 8–10 December 2003). Plasma Physics and Controlled Fusion, 2005, 47, 1351-1366.	0.9	0
161	Toroidal Plasma Rotation Induced by the Dynamic Ergodic Divertor in the TEXTOR Tokamak. Physical Review Letters, 2005, 94, 015003.	2.9	73
162	Flux dependence of carbon chemical erosion by deuterium ions. Nuclear Fusion, 2004, 44, L21-L25.	1.6	97

#	Article	IF	CITATIONS
163	Modelling of carbon transport in fusion devices: evidence of enhanced re-erosion of in-situ re-deposited carbon. Journal of Nuclear Materials, 2004, 328, 62-66.	1.3	56
164	Modeling of erosion and deposition patterns on C–W and W–Ta twin limiters exposed to the TEXTOR edge plasmas. Journal of Nuclear Materials, 2004, 329-333, 732-736.	1.3	8
165	The dynamic ergodic divertor in the TEXTOR tokamak: plasma response to dynamic helical magnetic field perturbations. Plasma Physics and Controlled Fusion, 2004, 46, B143-B155.	0.9	34
166	Influence of Methane Fuelling on the 2-D Line Radiation Distribution in the JET MkIIGB Divertor. Physica Scripta, 2004, T111, 101.	1.2	5
167	Deposition of Hydrogen Rich Carbon Films in Pump Ducts of TEXTOR. Physica Scripta, 2004, T111, 118.	1.2	9
168	Chemical Erosion Measurements in Tokamaks by Spectroscopy. Physica Scripta, 2004, T111, 42.	1.2	25
169	Modeling of Material Mixing Effects on Plasma Surface Interactions in Magnetic Fusion Devices. Physica Scripta, 2004, T111, 138.	1.2	12
170	Chemical erosion behaviour of carbon materials in fusion devices. Journal of Nuclear Materials, 2003, 313-316, 354-359.	1.3	20
171	Modelling of the transport of methane and higher hydrocarbons in fusion devices. Journal of Nuclear Materials, 2003, 313-316, 444-449.	1.3	14
172	An overview of JET edge modelling activities. Journal of Nuclear Materials, 2003, 313-316, 868-872.	1.3	10
173	Tomographic reconstruction of 2D line radiation distribution in the JET MkIIGB divertor. Journal of Nuclear Materials, 2003, 313-316, 925-930.	1.3	15
174	Short and long range transport of materials eroded from wall components in fusion devices. Journal of Nuclear Materials, 2003, 313-316, 311-320.	1.3	49
175	Advances in the modeling of chemical erosion/redeposition of carbon divertors and application to the JET tritium codeposition problem. Journal of Nuclear Materials, 2003, 313-316, 424-428.	1.3	24
176	Hydrocarbon transport in the MkIIa divertor of JET. Plasma Physics and Controlled Fusion, 2003, 45, 309-319.	0.9	27
177	Erosion and redeposition of wall material in controlled fusion devices. Vacuum, 2002, 67, 399-408.	1.6	56
178	Deposition and Erosion in Local Shadow Regions of TEXTOR-94. Physica Scripta, 2001, T94, 141.	1.2	9
179	Monte-Carlo Simulations of Chemical Erosion in TEXTOR-94 with the ERO-TEXTOR Code. Physica Scripta, 2001, T91, 57.	1.2	5
180	Investigation of carbon transport in the scrape-off layer of TEXTOR-94. Journal of Nuclear Materials, 2001, 290-293, 362-366.	1.3	55

#	Article	lF	CITATIONS
181	Modelling of erosion and deposition at limiter surfaces and divertor target plates. Journal of Nuclear Materials, 2001, 290-293, 238-244.	1.3	22
182	Comparison of impurity production, recycling and power deposition on carbon and tungsten limiters in TEXTOR-94. Journal of Nuclear Materials, 2001, 290-293, 276-280.	1.3	15
183	Operation of TEXTOR-94 with tungsten poloidal main limiters. Journal of Nuclear Materials, 2001, 290-293, 947-952.	1.3	42
184	Behaviour of Silicon-Doped CFC Limiter under High Heat Load in TEXTOR-94. Physica Scripta, 2001, T91, 61.	1.2	5
185	Graphite–tungsten twin limiters in studies of material mixing processes on high heat flux components. Journal of Nuclear Materials, 2000, 283-287, 1089-1093.	1.3	14
186	Simulation of the plasma-wall interaction in a tokamak with the Monte Carlo code ERO-TEXTOR. Nuclear Fusion, 2000, 40, 989-1001.	1.6	233
187	Investigation of Erosion and Deposition on Wall Components of TEXTOR-94. Physica Scripta, 1999, T81, 19.	1.2	16
188	Chemical Erosion in TEXTOR-94. Physica Scripta, 1999, T81, 48.	1.2	14
189	Experiments with tungsten limiters in TEXTOR-94. Journal of Nuclear Materials, 1998, 258-263, 858-864.	1.3	46
190	Understanding tungsten erosion during inter/intra-ELM periods in He-dominated JET-ILW plasmas. Physica Scripta, 0, , .	1.2	6